

GPU accelerated Trotter-Suzuki solver for quantum spin dynamics

Axel D. Dente* and Carlos S. Bederián, Pablo R. Zangara, Horacio M. Pastawski

*Instituto de Física Enrique Gaviola (CONICET) and Facultad de Matemática,
Astronomía y Física, Universidad Nacional de Córdoba,
Ciudad Universitaria, 5000, Córdoba, Argentina*

The resolution of dynamics in out of equilibrium quantum spin systems relies at the heart of fundamental questions among Quantum Information Processing, Statistical Mechanics and Nano-Technologies. Efficient computational simulations of interacting many-spin systems are extremely valuable tools for tackling such questions. Here, we use the Trotter-Suzuki (TS) algorithm, a well-known strategy that provides the evolution of quantum systems, to address the spin dynamics. We present a GPU implementation of a particular TS version, which has been previously implemented on single cores in CPUs. We develop a massive parallel version of this algorithm and compare the efficiency between CPU and GPU implementations. This boosted method reduces the execution time in several hundred times and is capable to deal with systems of up to 27 spins (only limited by the GPU memory).

* dente@famaf.unc.edu.ar

I. INTRODUCTION

The evolution of a generic quantum spin system is described by an appropriate Schrödinger equation, where the Hamiltonian operator \hat{H} encloses all the information about its dynamics, including external fields and spin-spin interactions. The “academic” strategy involves the solution of an eigen-problem for \hat{H} and the state vectors $|\psi\rangle$ [1]. This can be a major computational task, since the dimensionality of the underlying Hilbert space scales exponentially with the number N of interacting spins in the system. In practice, such scenario constrains the problem to the treatment of few-spins systems, or dealing with special cases where symmetries provide further simplifications [2].

As alternatives to the full matrix diagonalization, we recall strategies such as the Lanczos algorithm [3–5] and the Trotter-Suzuki (TS) algorithm [6, 7]. The Lanczos algorithm is usually employed in more sophisticated and well-known methods like the Density Matrix Renormalization Group [8, 9], which is a truncation of the Hilbert space to the specific energy excitations. However, it may be inadequate for dealing with high-temperature quantum systems, which is the case of spin dynamics (SD) relevant for Magnetic Resonance (MR)[10]. Recently, an algorithm based on the state space restriction approximation has been proposed for such a scenario [11]. This method relies on beforehand assumptions about spin environments, that provide a physically grounded Hilbert space truncation.

The TS algorithm divides the Hamiltonian operator into a sum of diagonal and non-diagonal terms. A full unitary evolution is built by successive (partial) short-time evolution operators, each arising from the Hamiltonian terms. Provided that the time steps are short enough, the exact evolution is well approximated by the successive partial evolutions. This method has been implemented on general purpose Graphics Processing Units (GPU) to simulate single particle dynamics when the Schrödinger equation is reduced into the tight-binding approximation [12, 13].

In this article we report the implementation of a 4th order TS decomposition for SD in GPU. We consider generic spin Hamiltonians without any Hilbert space truncation or any further assumption about symmetries or ad hoc dynamical conditions. Our implementation is based on the XYZ decomposition [14], in which the Hamiltonian is partitioned in the X, Y and Z components of the interactions bilinear in spin. Since the Z component can be written in a simple diagonal form, it only modifies the phases of the states. Moreover, X

and Y components are intrinsically non-diagonal, and thus local rotations are performed in order to map them into Z-like terms.

The Z-like terms and the local rotations are implemented by means of a massive parallelization scheme. The speedup obtained goes beyond 700 times compared with a single CPU core implementation. Despite this decrease in the execution time, the system size is still bounded by the maximum amount of memory available, which is about 6GB for current-generation GPUs. Thus, our implementation is capable to reach a system of 27 spins, which is still a significant number when compared to other methods.

The paper is organized as follows. In Sec. II we summarize the basis of the TS algorithm. In Sec. III we describe several implementations in GPUs, their performance and accuracy. We include also in A a brief discussion on two scenarios where this computational strategy can be employed: MR spin ensemble calculations, where the present work is up-to-date being exploited, and the potential use in the evolution of Matrix Product States. Sec. IV concludes the present work.

II. THE TROTTER-SUZUKI ALGORITHM

In this section we summarize the TS method for spin systems as presented in Ref. [7]. We start considering the following total spin Hamiltonian:

$$H = \sum_{j=1}^N \sum_{\alpha=x,y,z} h_j^\alpha S_j^\alpha + \sum_{j,k=1}^N \sum_{\alpha=x,y,z} J_{j,k}^\alpha S_j^\alpha S_k^\alpha, \quad (1)$$

where S_j^α is the spin operator at site j on axis $\alpha = x, y, z$. The parameters h_j^α define the local fields or chemical shifts, with the constrain $\langle h_j^\alpha \rangle \equiv 0$, while the $J_{j,k}^\alpha$ are the coupling between pair of spins.

We assume that the N -spin system is initially described by a state vector $|\Psi_0\rangle$, which is expanded in the computational Ising basis:

$$|\Psi_0\rangle = \sum_{i=1}^{2^N} c_i |\beta_i\rangle. \quad (2)$$

Here, c_i are complex coefficients and $|\beta_i\rangle$ are tensor products of eigenvectors of S_j^z operators, typically referred as the S^z -decoupled or *Ising* basis. In A we discuss two relevant cases in which *pure* states, as in Eq. 2, are employed to evaluate the dynamics in complex

many-body systems. In fact, we stress here that the present computational strategy can be substantially exploited when combined with sophisticated physically-based representations.

The state of the system at an arbitrary time t is formally given by $|\Psi_t\rangle = \mathbf{U}(t)|\Psi_0\rangle = e^{-itH/\hbar}|\Psi_0\rangle$. For simplicity, we set from now on $\hbar = 1$.

The main idea of the TS method relies on finding an appropriate partition of H which may yield a set of simple partial evolutions that approximate the exact one $\mathbf{U}(t)$. If we consider Eq. 1 as a particular sum of terms $H = H_1 + \dots + H_K$, then:

$$\mathbf{U}(t) = e^{-itH} = e^{-it(H_1+\dots+H_K)} = \lim_{m \rightarrow \infty} \left(\prod_k e^{-\frac{itH_k}{m}} \right)^m.$$

The first order approximation to $\mathbf{U}(t)$ is

$$\mathbf{U}(t) \simeq \tilde{\mathbf{U}}_1(t) = e^{-itH_1} \dots e^{-itH_K}, \quad (3)$$

while the second and fourth order approximations can be expressed in terms of the first:

$$\tilde{\mathbf{U}}_2(t) = \tilde{\mathbf{U}}_1^\dagger(-t/2)\tilde{\mathbf{U}}_1(t/2),$$

$$\tilde{\mathbf{U}}_4(t) = \tilde{\mathbf{U}}_2(at)\tilde{\mathbf{U}}_2(at)\tilde{\mathbf{U}}_2((1-4a)t)\tilde{\mathbf{U}}_2(at)\tilde{\mathbf{U}}_2(at),$$

where $a = 1/(4 - 4^{1/3})$. These are indeed satisfactory approximations to $\mathbf{U}(t)$ provided that t must be small enough compared to the maximum local time-scale determined by H . Such role is played by the local second moment of the interactions. This means that the partial evolution time step t must satisfy:

$$t \ll \left[\max_{j,k} \|H_{j,k}\| \right]^{-1} \simeq \left[\max_{j,k} \left[\sum_{\alpha=x,y,z} \left(\frac{h_j^\alpha}{2} \right)^2 + \sum_{\alpha=x,y,z} \left(\frac{J_{j,k}^\alpha}{4} \right)^2 \right]^{\frac{1}{2}} \right]^{-1} \quad (4)$$

Now we address specifically how to build an operator $\tilde{\mathbf{U}}_1(t)$ given by Eq. 3 from the total Hamiltonian of Eq. 1. The natural choice for the partition sum are the single-spin and the two-spin terms, which shall be mapped into a diagonal representation by suitable rotations. In particular, we consider the operators that rotate X and Y axis into the Z axis:

$$R_{\pi/2}^y = \frac{1}{\sqrt{2}} \begin{bmatrix} 1 & -1 \\ 1 & 1 \end{bmatrix}, R_{-\pi/2}^x = \frac{1}{\sqrt{2}} \begin{bmatrix} 1 & i \\ i & 1 \end{bmatrix}, \quad (5)$$

and satisfy:

$$(R_{\pi/2}^y)^\dagger S^x R_{\pi/2}^y = S^z,$$

$$(R_{-\pi/2}^x)^\dagger S^y R_{-\pi/2}^x = S^z.$$

These rotation operators are introduced to simplify the numerical computation, since the whole calculations are performed in the computational Ising basis, as mentioned above. For instance, the partial evolution $\exp[-it h_j^\alpha S_j^z]$ yields a trivial phase, while other cases shall be properly rotated using $R_{\pi/2,j}^y$ and $R_{-\pi/2,j}^x$. The j -index labels each spin, and the corresponding global rotations are defined by $Y = \bigotimes_j R_{\pi/2,j}^y$ and $X = \bigotimes_j R_{-\pi/2,j}^x$.

Let us first consider the single-spin operations,

$$\exp\left(-it \left[\sum_{j=1}^N \sum_{\alpha=x,y,z} h_j^\alpha S_j^\alpha \right]\right) \simeq \prod_{\alpha=x,y,z} \exp\left[-it \sum_{j=1}^N h_j^\alpha S_j^\alpha\right]. \quad (6)$$

Here, we stress that the approximate equality relies on the validity of Eq. 4. Non-trivial exponentials are rotated:

$$\begin{aligned} \exp\left[-it \sum_{j=1}^N h_j^x S_j^x\right] &= Y \exp\left(-it \sum_{j=1}^N h_j^x S_j^z\right) Y^\dagger, \\ \exp\left[-it \sum_{j=1}^N h_j^y S_j^y\right] &= X \exp\left(-it \sum_{j=1}^N h_j^y S_j^z\right) X^\dagger. \end{aligned} \quad (7)$$

Even though this kind of single-spin operations can in fact be computed exactly without rotations and without the approximation of Eq. 6, our purpose is to write all the partial evolution operators in an explicit diagonal form. This strategy will be specifically exploited in the computational implementation, as shown in Section III.

In analogy with Eq. 6, the two-spin operators yield:

$$\exp\left(-it \left[\sum_{j,k=1}^N \sum_{\alpha=x,y,z} J_{j,k}^\alpha S_j^\alpha S_k^\alpha \right]\right) \simeq \prod_{\alpha=x,y,z} \exp\left(-it \left[\sum_{j,k=1}^N J_{j,k}^\alpha S_j^\alpha S_k^\alpha \right]\right) \quad (8)$$

Once again, the Z-terms yield diagonal operators:

$$e^{itJ_{j,k}^z S_j^z S_k^z} = \begin{bmatrix} e^{itJ_{j,k}^z/4} & & & \\ & e^{-itJ_{j,k}^z/4} & & \\ & & e^{-itJ_{j,k}^z/4} & \\ & & & e^{itJ_{j,k}^z/4} \end{bmatrix}. \quad (9)$$

The remaining two-spin terms shall be rotated by Y and X accordingly,

$$\begin{aligned} \exp\left(-it \left[\sum_{j,k=1}^N J_{j,k}^\alpha S_j^x S_k^x \right]\right) &= Y \exp\left(-it \left[\sum_{j,k=1}^N J_{j,k}^x S_j^z S_k^z \right]\right) Y^\dagger, \\ \exp\left(-it \left[\sum_{j,k=1}^N J_{j,k}^\alpha S_j^y S_k^y \right]\right) &= X \exp\left(-it \left[\sum_{j,k=1}^N J_{j,k}^x S_j^z S_k^z \right]\right) X^\dagger. \end{aligned} \quad (10)$$

Notice that, from Eqs. 7 and 10, the rotations for single and double spin terms can be performed simultaneously.

III. IMPLEMENTATION AND RESULTS

Any state written in the form of Eq. 2 can be evolved by the successive application of partial evolution operators, as those defined in Sec. II. At any time, the state vector is represented by a double precision complex array that occupies $2^N \times 16$ bytes of memory. Its k th element stores the probability amplitude c_k for the corresponding basis (Ising) state. These basis states are tensor products of up and down configurations for each spin, and can be written according to the N -bit binary representation of k . Naturally, the size of the system is constrained by the maximum amount of memory available in the GPU (in our case, 6Gb for a Tesla C2070).

The implementation of the full evolution is divided into two main modules: phase-corrections and axis-rotations.

Forward Rotation \rightarrow Phases in $Z \rightarrow$ Backward Rotation

A. Phase correction

The first module performs the phase corrections depending on the Z -projection (up or down) and position of each spin in each state of the Ising basis (which are 2^N states). In this

stage there are no cross terms between different base states (all operations are diagonal), and hence the parallelization is trivial. However, due to the two-spin terms, the time of evaluation of each phase correction increases quadratically with the number of spins.

If the Hamiltonian is independent of time, then phase corrections can be computed previously, i.e. before performing the sequence of partial evolutions. In fact, Eq. 9 ensures that the phases only depend on the time step and the Hamiltonian parameters. The disadvantage of such pre-computed phase corrections relies on the amount of memory required, which is equivalent to that of the state vector. Thus, it increases the memory usage by 150%, limiting simulations to 27 spins on 6GB GPUs instead of 28, but reduces phase correction time by 97%.

Additionally, since every phase correction is followed by a backward rotation that also operates on the whole state, the phase correction kernel is merged with the backward rotation kernel. This means that phase correction is performed when the rotation kernel reads elements from memory and just before applying the rotation. This saves two global memory operations on each element and a kernel call.

Combined, these improvements reduce the overall simulation time by up to 52%.

B. Rotation

The rotation module acts over a pair of basis states by means of the operators defined in Eq. 5. If a particular basis state has the j -th spin down, then it is paired to the basis state that has the j -th spin up and the same configuration for the rest of spins:

$$\begin{aligned} n_{j,\downarrow} &= \dots \downarrow_j \dots \\ n_{j,\uparrow} &= \dots \uparrow_j \dots = n_{j,\downarrow} + 2^j. \end{aligned} \tag{11}$$

This pairing procedure must range the whole Hilbert space. Hence, for every value of j the pairing must be repeated over all the 2^{N-1} states that have the sought configuration in the j -th spin.

In order to show how the parallelization can be performed at this stage, let us exemplify one case of the pairing procedure. If we address the rotation of the second spin of a four-spin

system, then pairs of states under consideration are the following:

$$\begin{array}{cccccccc} \downarrow\downarrow\downarrow & \downarrow\downarrow\downarrow\uparrow & \downarrow\downarrow\uparrow\downarrow & \downarrow\downarrow\uparrow\uparrow & \uparrow\downarrow\downarrow\downarrow & \uparrow\downarrow\downarrow\uparrow & \uparrow\downarrow\uparrow\downarrow & \uparrow\downarrow\uparrow\uparrow \\ \downarrow\uparrow\downarrow\downarrow & \downarrow\uparrow\downarrow\uparrow & \downarrow\uparrow\uparrow\downarrow & \downarrow\uparrow\uparrow\uparrow & \uparrow\uparrow\downarrow\downarrow & \uparrow\uparrow\downarrow\uparrow & \uparrow\uparrow\uparrow\downarrow & \uparrow\uparrow\uparrow\uparrow \end{array} \text{ and } \begin{array}{c} \uparrow\downarrow\uparrow\uparrow \\ \uparrow\uparrow\uparrow\uparrow \end{array}.$$

From this example it is straightforward clear that there are no repetitions in any of the basis states when evaluating one specific rotation (for a particular j). Thus, each rotation operation within the same j -spin results independent and can be parallelized.

C. Efficient rotation on GPUs

Since each rotation is independent (fixed j), we initially wrote a GPU kernel that rotates the j -th spin on a single pair and launched 2^{N-1} threads, one per pair. However, as each individual rotation is computationally cheap, the kernel is limited by memory bandwidth to feed each thread with its pair of states. To avoid this bottleneck, we aim to read each of these states from memory and perform as many rotations as is possible before writing them back to memory.

If we take any subset of spins $F \in \mathcal{P}(\{1..N\})$ and fix their positions to $\{f_i | i \in F\}$, then the set of all states that satisfy these restrictions $\{s = s_0s_1..s_n | \forall i \in F : s_i = f_i\}$ is closed under the state pairing function that flips any spin that is not in F . This allows us to launch $2^{|F|}$ thread blocks, and set the spin positions f_i using the binary encoding of each thread block's unique index. This leaves each thread block with its own set of $2^{N-|F|}$ states to rotate and, by its construction, every state's peers for spins $\{1..N\} - F$ are also within the set. Thus, each thread block copy its states to the fast shared memory available in each multiprocessor within a GPU, and perform the rotations for all the spins in $\{1..N\} - F$ without performing any further global memory accesses. Once these rotations are done, the results are copied back to global memory and the kernel ends.

While this technique improves rotation times, the approach has a problem: when rotating higher spins, the lower bits of the state indices handled by a thread block are given by the block index, which results in adjacent states being interleaved across different thread blocks. For example, when rotating spins 4 and 5 in a single kernel call on a 5-spin problem, the set of states of thread block 0 would be $\{00000_b = 0; 01000_b = 8; 10000_b = 16; 11000_b = 24\}$, thread block 1 would be $\{00001_b = 1; 01001_b = 9; 10001_b = 17; 11001_b = 25\}$, and so on. As

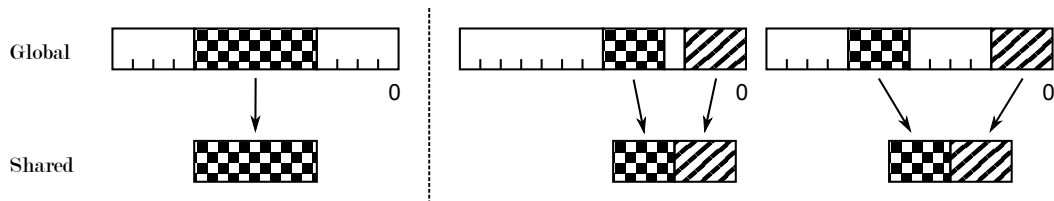


FIG. 1. Rotation of spins 4 through 9 using both multiple rotation kernels. The clear bits are set by the thread block index, while the striped and checkered spins are set within each block. Checkered spins are rotated in shared memory.

GPU memory controllers are built for fetching lines of contiguous data, currently 128 bytes long, this interleaving wastes memory bandwidth significantly.

To solve this problem, when rotating over higher spins we shift thread block indices a number of bits s to the left, and each thread block must contain the states for every combination of these s lower bits. While this means that the kernel rotates s fewer spins per run, it also arranges states into groups of 2^s contiguous elements in memory. Continuing with the previous example, if we had a shift of one element then thread block 1 would handle states $\{00010_b = 2; 00011_b = 3; 01010_b = 10; 01011_b = 11; 10010_b = 18; 10011_b = 19; 11010_b = 26; 11011_b = 27\}$. The improved memory bandwidth efficiency results in a further improvement of about 300% over the previous kernel for $s = 3$, which matches the memory controller's 128 bytes line length.

As we measured rotation times for different values of s and different thread block sizes, we noticed that there are not optimal values that work for every rotation and every system size. Thus, we implement a minimization algorithm which searches the optimal value for each system size and records such configuration. This recorded setup is used in every running of the TS algorithm which uses the same GPU card.

D. Speedup

As a result of this implementation we plot in Fig. 2 the execution times for the CPU and each of the three GPU versions. At this point it is necessary to stress that the CPU version is not so tuned as the GPU implementations. However, it is shown with the purpose to remark the overall improvement obtained with the use of the GPU.

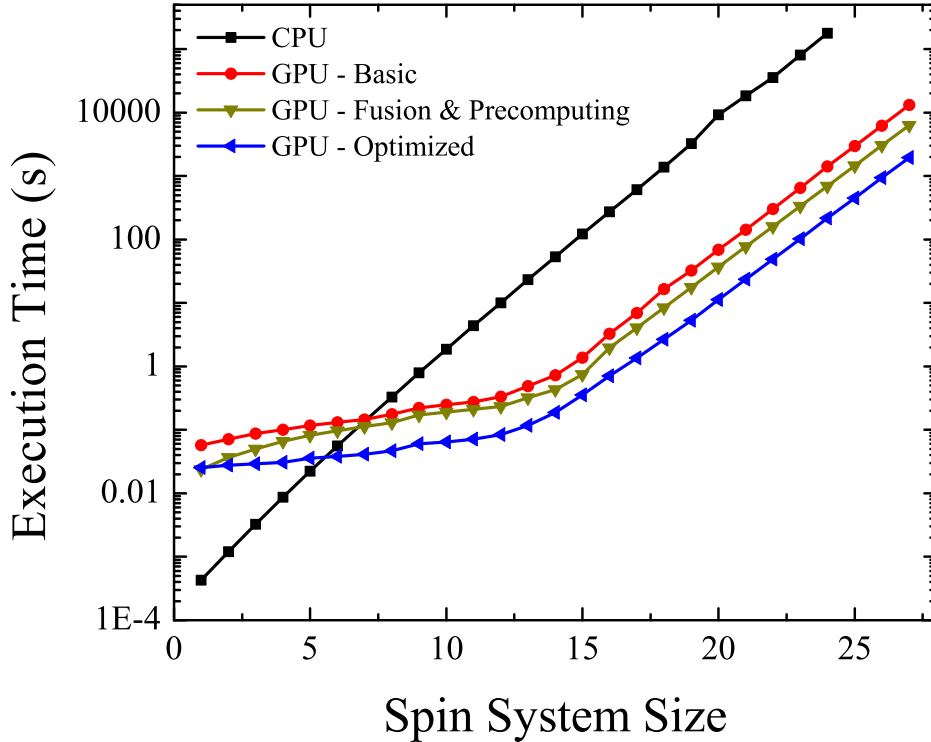


FIG. 2. Execution time (in logarithmic scale) for CPU and three GPU implementations of the Trotter-Suzuki method as a function of the number of spins. Each point correspond to the evolution with 50 Trotter-Suzuki steps. For low number of spins ($N \leq 5$) the CPU-version has better performance than the GPU, while for $N > 5$ the GPU versions dominates showing an increase of performance that exceeds more than one hundred times the CPU version

From Fig. 2, for small systems ($N \leq 5$), it is observed that the CPU is faster than any GPU implementation. This behavior is consistent with the fact that for these sizes the problem fits into the cache memory of the CPU processor. Thus, the high memory bandwidth makes the algorithm to run faster than any GPU version. Additionally, the smooth growth observed in Fig. 2 for $N < 15$ in the GPU versions, indicates that the GPU does not fill its full capability. Hence, the maximum efficiency in the GPU is not reached and the difference between the CPU and GPU progressively grows.

In the opposite case, when N is considerably large, the execution time of the GPU implementation increases exponentially. The inflection point around $N \simeq 14$ indicates that the GPU reaches its full capacity, and afterwards each GPU version scales as α^N , with a factor

α higher than 2. In Fig. 3-a and b we plot the speedup of selected implementations. The α parameter can be obtained by fitting linearly each curve for $N > 14$. We note that α is higher than 2 and the exact value depends on the algorithm version. For the CPU case we obtain $\alpha = 2.20$, meanwhile for the GPU-Basic case $\alpha = 2.11$ and for the GPU-Optimized version $\alpha = 2.09$. These small differences between the implementations are reflected in the behavior of the speedup. As it is shown in Fig. 3, the speedup grows with the system size, evidencing the differences of the α parameters.

It is worthy to stress the performance obtained with the GPU implementations, one of them without optimization at all (GPU-Basic) and the other a fully optimized version. In the first case, we observe a speedup of 73 times as compared to the CPU version (we consider $N = 14$ for reference). In the second case, i.e. the optimized one, the speedup reaches almost 290 times. In terms of spin systems, this allows the evaluation of systems which have 8 extra spins in the same computational time.

E. Accuracy

The last issue to be addressed concerns to the accuracy of our TS implementation. Several comparisons were performed between the present method and exact diagonalization schemes [15–17], i.e. the solution of the Schrödinger equation as an eigenproblem. The evolution of local and non-local physical magnitudes was compared, for one-dimensional spin systems described by Hamiltonians in the form of Eq. 1. For $N = 16$ [18], a sequence of 5×10^6 TS steps yields a relative difference bounded by 10^{-8} . A second accuracy test was provided by the spurious total magnetization observed in polarization-conserving Hamiltonians. In fact, this is a strictly physical condition: if the initial state has zero total magnetization, then the evolved one should remain so. In general, we observe a linear increase of the total magnetization of the spin system, which is consistent with the general expectancies of a linear increase of the TS error as function of the number of steps. In particular, for $N = 22$ and 5×10^6 TS steps, we observe a relative deviation less than 10^{-6} , a precision which is good enough for practical purposes.

An alternative strategy for error quantification is provided by the *Loschmidt echo* (LE) [19]. It evaluates the reversibility of a system’s dynamics in the presence of uncontrolled degrees of freedom [20]. For a particular initial state $|\Psi_0\rangle$, the standard LE definition [21]

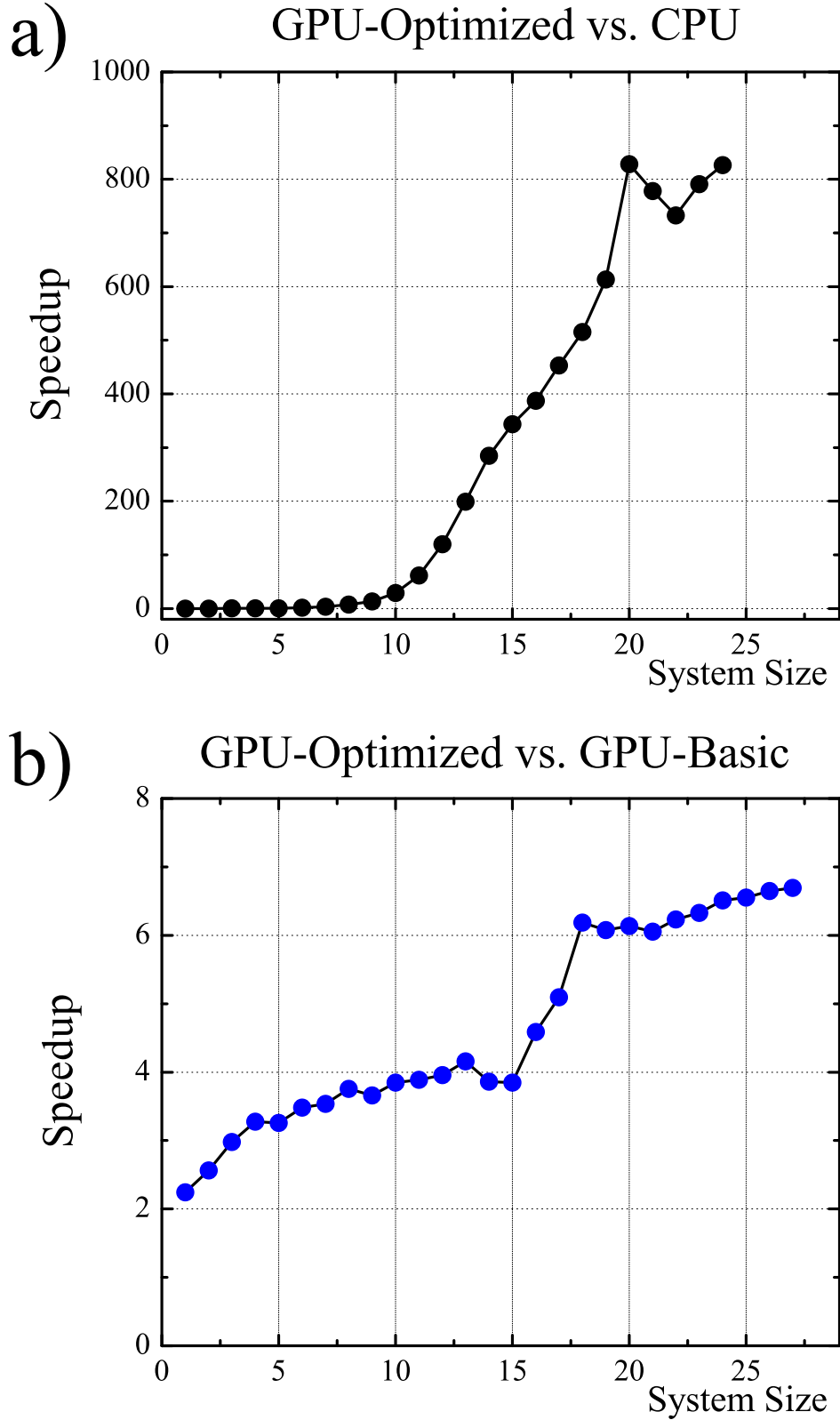


FIG. 3. Speedup between the implementations. **a**: CPU vs GPU-Optimized. For large spin systems the GPU is about 800 times faster than the CPU. **b**: Optimized GPU version versus the basic implementation in the GPU. It is observed an increase greater than 6 times for long spin

is:

$$M_{LE}(2t) = |\langle \Psi_0 | \exp [i(H_0 + \Sigma)t] \exp [-iH_0t] | \Psi_0 \rangle|^2, \quad (12)$$

where H_0 is a reversed Hamiltonian, and Σ encloses uncontrolled non-reversed degrees of freedom. In the present case, we set $\Sigma \equiv 0$, which for an ideal perfectly accurate computation would yield $M_{LE} \equiv 1, \forall t$. In principle, this statement is completely irrespective of the TS approximation and its intrinsic accuracy (i.e. the validity of Eq. 4). As a matter of fact, exactly the same sequences of TS partial evolutions are applied in the forward and backwards dynamics, except for the change in the sign of t . Therefore, the deviations of M_{LE} away from the unity could be intrinsically originated in the execution of floating point operations by the specific Hardware.

We consider initial states given by random superpositions of Ising states (e.g. Eq. A2), for a $N = 16$ spin set. Two cases of different dynamical complexity are evaluated. The first case is a ring configuration described by a nearest neighbors Heisenberg Hamiltonian. As above, this interaction conserves total magnetization, and then the dynamics does not explore the whole Hilbert space. For this case, 5×10^5 TS steps yield $|1 - M_{LE}| = 5.206647 \times 10^{-8}$, while 5×10^6 TS steps yield $|1 - M_{LE}| = 5.2066504 \times 10^{-7}$. Again, the error appears to increase linearly with the number of TS steps. However, we stress here that these deviations cannot be associated to the TS decomposition. The second case is built from the first, adding double quantum terms $S_j^x S_k^x - S_j^y S_k^y$ up to third next nearest neighbors. In this situation, total magnetization is not conserved, and therefore dynamics effectively mixes all spin projection subspaces exploring the whole Hilbert space. It turns out that 5×10^6 TS steps yield $|1 - M_{LE}| = 5.2094531 \times 10^{-7}$, which is slightly larger than the first case. This may indicate that errors in computational operations can depend on the complexity of the many-body dynamics.

Once again, these examples evidence a satisfactory accuracy of our TS-GPU implementation. A systematic study of the LE as an error quantifier is well beyond the scope of this article. This would require ranging over N and the number of TS steps, different Hamiltonian complexities and initial states, among many other factors. However, the LE turns to be a promising witness to address computational errors in GPU and CPU implementations.

IV. CONCLUSIONS

We presented here a GPU implementation that boosted the Trotter-Suzuki method for quantum spin dynamics. We developed a parallelization scheme to exploit the massive parallel architecture of the GPU cards. The results showed a significant increase of performance (which can reach more than one hundred times) as compared with the single CPU core implementation.

Additionally, we showed several upgrades in the GPU versions that yield an extra speedup of 6 times for large spin systems. The benefits enabled by this massive parallel hardware, boosted the capability of evaluating the dynamics of considerably large quantum spin systems. In particular, we were able to evolve a maximum of 27 spins (limited only by the GPU memory) in reasonable execution times.

The comparison between our Trotter-Suzuki implementation with exact numerical approaches yielded estimated relative errors, which turned to be fairly acceptable within the standard expectancies of this kind of computational strategy.

The implementation of this algorithm and the efficiency achieved, open promising opportunities for studying fundamental questions within the field of out-of-equilibrium quantum many-body systems.

V. ACKNOWLEDGEMENTS

The authors acknowledge Lea F. Santos for providing the data for accuracy comparison, and Nicolás Wolovick for fruitful discussions. This work was performed with the financial support from CONICET, ANPCyT, SeCyT-UNC, MinCyT-Cor, and the NVIDIA professor partnership program.

Appendix A: Spin systems described by single pure states

We will briefly mention here two cases where an interacting many-spin system \mathcal{S} can be described or approximately described by, a pure state: the random superposition (entangled) states for high temperature systems, and the so-called Matrix Product States. These are suited candidates for our GPU-boosted TS implementation.

In the first case, \mathcal{S} is characterized by the infinite temperature limit, as it is often the situation in Magnetic Resonance spin dynamics. Strictly speaking, \mathcal{S} cannot be described by a pure (single vector) state as in Eq. 2, but by a highly mixed state, typically denoted by a density matrix. This represents a whole probabilistic ensemble, and contains all the statistical information about \mathcal{S} [22]. The manipulation of the density matrix may rapidly be cumbersome due to memory requirements, as soon as its dimension scales as $2^N \times 2^N$. But, provided the observables to be evaluated are local (they involve just a few spins within \mathcal{S}), one can use just a few pure entangled states to compute ensemble-averaged quantities [23]. This procedure enables a physical parallelization which relies on the quantum superposition principle. A simple case may be an initial state given by a single spin up-polarized (localized excitation), and the rest of them in the high-temperature thermal equilibrium, represented by a mixture of all states with amplitudes satisfying the appropriate statistical weights and random phases:

$$|\Psi_0\rangle = |\uparrow\rangle_1 \otimes \left\{ \sum_{j=1}^{2^{N-1}} \frac{1}{\sqrt{2^{N-1}}} e^{i\varphi_j} |\beta_j\rangle \right\}, \quad \varphi_j = \text{random phase}, \quad (\text{A1})$$

where, analogously to Eq. 2, $|\beta_j\rangle$ are the states of the computational Ising basis. This case has been employed to evaluate specific time-dependent correlation functions for spin systems [20, 24, 25], avoiding the storage, manipulation and diagonalization of overwhelmingly large matrices. Most importantly, it is nowadays employed to address the problem of thermalization in closed quantum systems, being assisted with our GPU implementation.

The second case, refers to Matrix Product States [26, 27], which constitute a set of states that successfully approximates the exact state of \mathcal{S} in many physical situations. They are intimately related to renormalization group methods[9], and have proved very useful to deal with dynamical observables in one-dimensional quantum spin systems[28].

For a chain of N spins, a Matrix Product State is given by:

$$|\Psi_0\rangle = \sum_{i_1, \dots, i_N = \uparrow, \downarrow} \text{tr}(A_1^{i_1} \dots A_N^{i_N}) |i_1, \dots, i_N\rangle \quad (\text{A2})$$

where A_k^i is a D -dimensional matrix, and $|i_1, \dots, i_N\rangle$ represents an Ising state. The time-evolution of this kind of states is performed by a suitable TS algorithm[28], and therefore they are promising candidates for TS-GPU implementations like the one we present in this

article.

- [1] E. Merzbacher, *Quantum Mechanics* (Wiley, New York, 1998).
- [2] E. Lieb, T. Schultz, and D. Mattis, *Annals of Physics* **16**, 407–(1961).
- [3] C. Leforestier, R. Bisseling, C. Cerjan, M. Feit, R. Friesner, A. Guldborg, A. Hammerich, G. Jolicard, W. Karrlein, H.-D. Meyer, N. Lipkin, O. Roncero, and R. Kosloff, *Journal of Computational Physics* **94**, 59–(1991).
- [4] T. J. Park and J. C. Light, *The Journal of Chemical Physics* **85**, 5870–(1986).
- [5] J. Jaklič and P. Prelovšek, *Phys. Rev. B* **49**, 5065–(1994).
- [6] H. De Raedt and B. De Raedt, *Phys. Rev. A* **28**, 3575–(1983).
- [7] H. De Raedt and K. Michielsen, *Handbook of Theoretical and Computational Nanotechnology* (American Scientific Publishers, Los Angeles, 2006).
- [8] K. A. Hallberg, *Advances in Physics* **55**, 477–(2006), <http://www.tandfonline.com/doi/pdf/10.1080/00018730600766432>.
- [9] S. R. White, *Phys. Rev. Lett.* **69**, 2863–(1992).
- [10] C. P. Slichter, *Principles of magnetic resonance; 2nd ed.*, Springer series in solid state sciences (Springer, Berlin, 1980).
- [11] A. Karabanov, I. Kuprov, G. T. P. Charnock, A. van der Drift, L. J. Edwards, and W. Kockenberger, *The Journal of Chemical Physics* **135**, 084106(2011).
- [12] C. S. Bederián and A. D. Dente, *Proceedings of HPCLatAm 2011: High-Performance Computing Symposium* **40**, 63–(2011).
- [13] P. Wittek and F. M. Cucchiatti, *Computer Physics Communications* **184**, 1165–(2013).
- [14] H. De Raedt, A. Hams, K. Michielsen, and K. De Raedt, *Computer Physics Communications* **132**, 28–(1999).
- [15] K. Joel, D. Kollmar, and L. F. Santos, *ArXiv e-prints* (2012), arXiv:1209.0115 [cond-mat.stat-mech].
- [16] L. F. Santos, F. Borgonovi, and F. M. Izrailev, *Physical Review Letters* **108**, 094102(2012), arXiv:1110.4663 [quant-ph].
- [17] L. F. Santos, private communication(2013).
- [18] Standard exact diagonalization is limited by the size of systems that can be handled.

- [19] D. Wisniacki, A. Goussev, R. Jalabert, and H. Pastawski, *Scholarpedia* **7**, 11687–(2012).
- [20] P. R. Zangara, A. D. Dente, P. R. Levstein, and H. M. Pastawski, *Phys. Rev. A* **86**, 012322–(2012).
- [21] R. A. Jalabert and H. M. Pastawski, *Phys. Rev. Lett.* **86**, 2490–(2001).
- [22] K. Blum, *Density Matrix Theory and Applications*, Physics of Atoms and Molecules (Plenum Press, New York, 1996).
- [23] G. A. Álvarez, E. P. Danieli, P. R. Levstein, and H. M. Pastawski, *Phys. Rev. Lett.* **101**, 120503–(2008).
- [24] G. A. Álvarez, E. P. Danieli, P. R. Levstein, and H. M. Pastawski, *Phys. Rev. A* **82**, 012310–(2010).
- [25] T. A. Elsayed and B. V. Fine, *ArXiv e-prints* (2012), arXiv:1208.4652 [cond-mat.stat-mech].
- [26] M. Fannes, B. Nachtergaele, and R. Werner, *Communications in Mathematical Physics* **144**, 443–(1992).
- [27] M. C. Bañuls, M. B. Hastings, F. Verstraete, and J. I. Cirac, *Phys. Rev. Lett.* **102**, 240603–(2009).
- [28] A. Müller-Hermes, J. I. Cirac, and M. C. Bañuls, *New Journal of Physics* **14**, 075003–(2012).